Journal of Macromolecular Science, Part A
Publication details, including instructions for authors and subscription information:
http://www.informaworld.com/smpp/title~content=t713597274

Assessing the Importance of Diffusion-Controlled Effects on Polymerization Rate and Molecular Weight Development in Nitroxide-Mediated Radical Polymerization of Styrene

Martha Roa-Luna[a]; Martha Patricia Díaz-barber[a]; Eduardo Vivaldo-Lima[ab]; Liliane M. F. Lona[c]; Neil T. McManus[b]; Alexander Penlidis[b]
[a] Departamento de Ingeniería Química, Facultad de Química, Universidad Nacional Autónoma de México (UNAM), Conjunto E, Ciudad Universitaria, México, D. F., México [b] Institute for Polymer Research (IPR), Department of Chemical Engineering, University of Waterloo, Waterloo, Ontario, Canada [c] Faculdade de Engenharia Química, Departamento de Processos Químicos, Universidade Estadual de Campinas, Campinas, São Paulo, Brazil

To cite this Article Roa-Luna, Martha , Díaz-barber, Martha Patricia , Vivaldo-Lima, Eduardo , Lona, Liliane M. F. , McManus, Neil T. and Penlidis, Alexander(2007) 'Assessing the Importance of Diffusion-Controlled Effects on Polymerization Rate and Molecular Weight Development in Nitroxide-Mediated Radical Polymerization of Styrene', Journal of Macromolecular Science, Part A, 44: 2, 193 — 203
To link to this Article: DOI: 10.1080/10601320601031366
URL: http://dx.doi.org/10.1080/10601320601031366

Journal of Macromolecular Science ®, Part A: Pure and Applied Chemistry (2007) **44**, 193–203

ISSN: 1060-1325 print/1520-5738 online
DOI: 10.1080/10601320601031366

Assessing the Importance of Diffusion-Controlled Effects on Polymerization Rate and Molecular Weight Development in Nitroxide-Mediated Radical Polymerization of Styrene

MARTHA ROA-LUNA,[1] MARTHA PATRICIA DÍAZ-BARBER,[1] EDUARDO VIVALDO-LIMA†,[1,2] LILIANE M.F. LONA,[3] NEIL T. MCMANUS,[2] and ALEXANDER PENLIDIS[2]

[1]*Departamento de Ingeniería Química, Facultad de Química, Universidad Nacional Autónoma de México (UNAM), Conjunto E, Ciudad Universitaria, México, D. F., México*
[2]*Institute for Polymer Research (IPR), Department of Chemical Engineering, University of Waterloo, Waterloo, Ontario, Canada*
[3]*Universidade Estadual de Campinas, Faculdade de Engenharia Química, Departamento de Processos Químicos, Campinas, São Paulo, Brazil*

Received July, 2006, Accepted July, 2006

A previously derived kinetic model for the nitroxide-mediated radical polymerization (NMRP) of styrene has been modified by considering diffusion-controlled (DC) effects on the bimolecular radical termination, monomer propagation, dormant polymer activation, and polymer radical deactivation reactions. Free-volume theory was used to incorporate the DC-effects into the model. It was found that DC-termination enhances the living behavior of the system, whereas DC-propagation, DC-activation and DC-deactivation worsen it. Although the inclusion of overall DC-effects into the kinetic model improved the performance of the model by slightly reducing the deviations obtained from experimental data of polymerization rate and molecular weight in the bimolecular NMRP of styrene with 2,2,6,6-tetramethyl-1-piperidinyloxy (TEMPO) and dibenzoyl peroxide (BPO), it does not seem to justify adding the extra four free-volume parameters. In the case of the semi-batch addition of azo-bis-iso-butyronitrile (AIBN) (several single shots at definite time intervals) in the NMRP of styrene, recently reported in the literature, it was found that DC effects are more significant, but it was observed that there was a strong dependence of polymerization rate on the frequency of addition of the shots of initiator (a maximum on polymerization rate being observed at a given frequency of addition of the shots), which could not be adequately explained in terms of DC-effects.

Keywords: living radical polymerization; controlled radical polymerization; polystyrene; mathematical modeling; diffusion-controlled effects; TEMPO

1 Introduction

Nitroxide-mediated radical polymerization (NMRP) is one of the most advanced areas of controlled/living radical polymerization (CLRP). Well-defined block and graft copolymers, gradient and periodic copolymers, stars, combs, polymer networks, end-functional polymers and many other materials can be synthesized using CLRP technology (1). These materials find uses as coatings, adhesives, surfactants, dispersants, lubricants, gels, additives and thermoplastic elastomers, as well as in many electronic and biomedical applications (1). Stabilizers synthesized by NMRP are already being produced at the industrial scale (2–4).

The literature on the polymer chemistry of NMRP, centered on the design and synthesis of more effective controllers, has been reviewed by Hawker (5), and the kinetics of living radical polymerization, including NMRP, has been reviewed by the Fukuda group (6, 7). The kinetic/mechanistic understanding of NMRP, considering the quasi-steady state (QSS) of living radicals and the quasi-equilibrium (QSE) of persistent radicals, is at a very advanced stage (6–15). When side reactions not considered in the standard reaction mechanism of NMRP or polymerization conditions outside the theoretical bounds imposed by the QSS approach are taken into account, it is more convenient to use complete mathematical models, based on detailed reaction mechanisms (including the specific side reactions) and solved without the QSS or QSE assumptions,

†On research leave from UNAM
Address correspondence to: Eduardo Vivaldo-Lima, Departamento de Ingeniería Química, Facultad de Química, Universidad Nacional Autónoma de México (UNAM), Conjunto E, Ciudad Universitaria, México, D. F., CP 04510, México. Fax: (5255) 5622-5355. E-mail: vivaldo@servidor.unam.mx

such as the ones proposed by Zhang and Ray (16) and Bonilla et al. (17).

Diffusion-controlled (DC) effects have been considered in the modeling of CLRP by some authors in order to explain some deviations with respect to polymerization rate and molecular weight development. In the case of NMRP, empirical correlations, only for gel-effect, have been used (16, 18, 19). DC effects on the propagation, activation and deactivation, as well as termination reactions have been modeled using free-volume theory in the cases of INIFERTER polymerization (20), atom-transfer radical polymerization (ATRP) (21), and reversible addition-fragmentation transfer polymerization (RAFT) (22, 23). It has been proposed that DC-effects in the propagation, termination, activation and deactivation reactions can explain the acceleration in polymerization rate when AIBN is added in a semi-batch fashion (equally-spaced discrete shots of initiator) in the NMRP of styrene (24). However, in the previous study, very few simulations and limited discussion on the topic were offered.

In this contribution, the detailed kinetic model for NMRP proposed by Bonilla et al. (17) is modified to include DC-effects in all the reactions involving polymer molecules (bimolecular radical termination, monomer propagation, dormant polymer activation and polymer radical deactivation), using the free-volume theory. Parameter sensitivity analyses on the effect of the free-volume parameters on polymerization rate and molecular weight development are offered. The model predictions are compared against experimental data of bimolecular NMRP of styrene using TEMPO and BPO, and bimolecular NMRP of styrene using TEMPO and AIBN, with the semi-batch addition of the initiator (24).

2 Experimental

The experimental data for the bimolecular NMRP of styrene using TEMPO and BPO at a molar ratio of [TEMPO]/[BPO] = 1.1 and T = 120°C, used in the first case study of this paper, were generated in our group (25, 26).

The experimental data for the bimolecular NMRP of styrene using TEMPO and AIBN (added in a semi-batch fashion) at a molar ratio of [TEMPO]/[BPO] = 1.1 and T = 120°C, used in the second case study addressed in this paper, were taken from Díaz-Camacho et al. (24).

3 Modeling

The polymerization mechanism and kinetic model used in this paper are the same as those proposed by Bonilla et al. (17). The polymerization mechanism is shown in Table 1. All the kinetic rate constants used in the calculations presented in this study are listed in Table 2. With the exception of the initiator efficiency, f, and the kinetic rate constant of the enhancement reaction, k_{h3}, which were used as fitting parameters in some situations, all the remaining kinetic rate constants were fixed and taken from the literature.

Table 1. Polymerization Mechanism (17)

Description	Step
Chemical initiation	$I \xrightarrow{k_d} 2R^{\bullet}_{in}$
Mayo dimerization	$M + M \xrightarrow{k_{dim}} D$
Thermal initiation	$M + D \xrightarrow{k_{th}} D^{\bullet} + M^{\bullet}$
First propagation (primary radicals)	$R^{\bullet}_{in} + M \xrightarrow{k_i} R^{\bullet}_1$
First propagation (monomeric radicals)	$M^{\bullet} + M \xrightarrow{k_i} R^{\bullet}_1$
First propagation (dimeric radicals)	$D^{\bullet} + M \xrightarrow{k_i} R^{\bullet}_1$
Propagation	$R^{\bullet}_r + M \xrightarrow{k_i} R^{\bullet}_{r+1}$
Dormant living exchange (monomeric alkoxyamine)	$M^{\bullet} + NO^{\bullet}_x \underset{k_a}{\overset{k_{da}}{\rightleftharpoons}} MNO_x$
Dormant living exchange (polymeric alkoxyamine)	$R^{\bullet}_r + NO^{\bullet}_x \underset{k_a}{\overset{k_{da}}{\rightleftharpoons}} R_rNO_x$
Alkoxyamine decomposition	$MNO_x \xrightarrow{k_{decomp}} M + HNO_x$
Rate enhancement reaction	$D + NO^{\bullet}_x \xrightarrow{k_{h3}} D^{\bullet} + HNO_x$
Termination by combination	$R^{\bullet}_r + R^{\bullet}_s \xrightarrow{k_{tc}} P_{r+s}$
Termination by disproportionation	$R^{\bullet}_r + R^{\bullet}_s \xrightarrow{k_{td}} P_r + P_s$
Transfer to monomer	$R^{\bullet}_r + M \xrightarrow{k_{fm}} P_r + M^{\bullet}$
Transfer to dimer	$R^{\bullet}_r + D \xrightarrow{k_{fD}} P_r + D^{\bullet}$

The model equations for the batch case were solved with a self developed Fortran code (27). The Predici® commercial software was also used to simulate the different polymerization conditions studied in the paper, including all the simulations related to the semi-batch addition of AIBN. The profiles produced with our Fortran code for the batch case overlapped with the profiles produced with Predici®.

Diffusion controlled effects on the propagation, bimolecular radical termination, dormant polymer activation, and polymer radical deactivation reactions were modeled using the free-volume theory (20–22, 24, 32). The expressions used for the conversion-dependent kinetic rate constants of these reactions are summarized in Table 3. v_f in the equations of Table 3 is the fractional free-volume, whereas v_{f0} is the fractional free volume at initial conditions. The free volume parameters, β_t, β_p, β_a, and β_d are "overlap" factors for the termination, propagation, activation, and deactivation reactions, respectively. These overlap factors account for the fact that the same free-volume is available to several molecules. They also account for molecule separation, once the molecules are in close proximity, but have not yet reacted (32). T and T_{gi} are reaction temperature and glass transition temperature of component i, respectively; and α_i is the expansion coefficient for species i. V_i and V_t are volume of species i and total system volume, respectively.

Table 2. Kinetic parameters used in the model

Parameter	Units	Value or function	Reference
k_i (BPO)	s^{-1}	$1.7 \times 10^{15} \exp\left(-\frac{30000}{RT}\right)$; $6.94 \times 10^{13} \exp\left(-\frac{29229}{RT}\right)$	(16) (Figs. 1–5) (28) ("alternate" in Fig. 5)
k_{di} (AIBN)	s^{-1}	$2.89 \times 10^{15} \exp\left(-\frac{31122}{RT}\right)$	(28)
f (BPO)		0.55 (0.1)	16 (see discussion about the "alternate" profiles of Fig. 5)
f (AIBN)		0.461	
k_{dim}	L mol^{-1} s^{-1}	$188.97 \exp\left(-\frac{16185.1}{RT}\right)$	(27)
k_i	L mol^{-1} s^{-1}	$6.359 \times 10^{12} \exp\left(-\frac{36598.55}{RT}\right)$	(27)
k_{p0}	L mol^{-1} s^{-1}	2050	(29)
k_{tc0}	L mol^{-1} s^{-1}	3.34×10^8	(30)
k_{fM}	L mol^{-1} s^{-1}	0	Neglected
k_{fD}	L mol^{-1} s^{-1}	0.0	Neglected
k_{da}	L mol^{-1} s^{-1}	4.7905×10^7	Assuming the same equilibrium constant (K) at 125°C of ref. 8
k_a	s^{-1}	$3 \times 10^{13} \exp\left(-\frac{29634}{RT}\right)$	(31)
k_{decomp}	s^{-1}	$5.7 \times 10^{14} \exp\left(-\frac{36639.6}{RT}\right)$	(16)
k_{h3}	L mol^{-1} s^{-1}	0.001 (0.01)	(17, 27)

4 Results and Discussion

The bimolecular NMRP of styrene at 120°C using TEMPO and BPO at a molar ratio TEMPO/BPO of 1.1 was used as a reference case in the first part of this study. Parameter sensitivity analyses on the effects of the free-volume parameters (DC-effects) on polymerization rate and molecular weight development, as well as comparison of model predictions (with and without DC-effects) against experimental data generated in our own group (25, 26) are presented in subsection 4.1.

In the second part, the NMRP of styrene at 120°C using TEMPO and AIBN (added in a semi-batch fashion), in a range of TEMPO/AIBN ratios between 0.87 and 1.8 is studied. A much more detailed simulation study than the one reported in Díaz-Camacho et al. (24), is presented in the second part of our study (subsection 4.2). A comparison of model predictions against selected experimental data from Díaz-Camacho et al. (24) is also offered in that subsection.

Table 3. Mathematical expressions for diffusion-controlled (DC) effects

Reaction or variable	Mathematical expression	Comments
Monomer propagation	$k_p = k_p^0 \exp\left[-\beta_p\left(\frac{1}{V_f} - \frac{1}{V_{f0}}\right)\right]$	
Bimolecular termination	$k_{tjn} = k_{tj}^0 \exp\left[-\beta_t\left(\frac{1}{V_f} - \frac{1}{V_{f0}}\right)\right]$, $j = c, d$	"c" stands for combination, and "d" for disproportionation
Dormant polymer activation	$k_a = k_a^0 \exp\left[-\beta_a\left(\frac{1}{V_f} - \frac{1}{V_{f0}}\right)\right]$	
Living polymer deactivation	$k_{da} = k_{da}^0 \exp\left[-\beta_d\left(\frac{1}{V_f} - \frac{1}{V_{f0}}\right)\right]$	
Fractional free volume	$v_f = \sum_{i=1}^{\#\text{ of components}} [0.025 + \alpha_i(T - T_{gi})] \frac{V_i}{V_t}$	

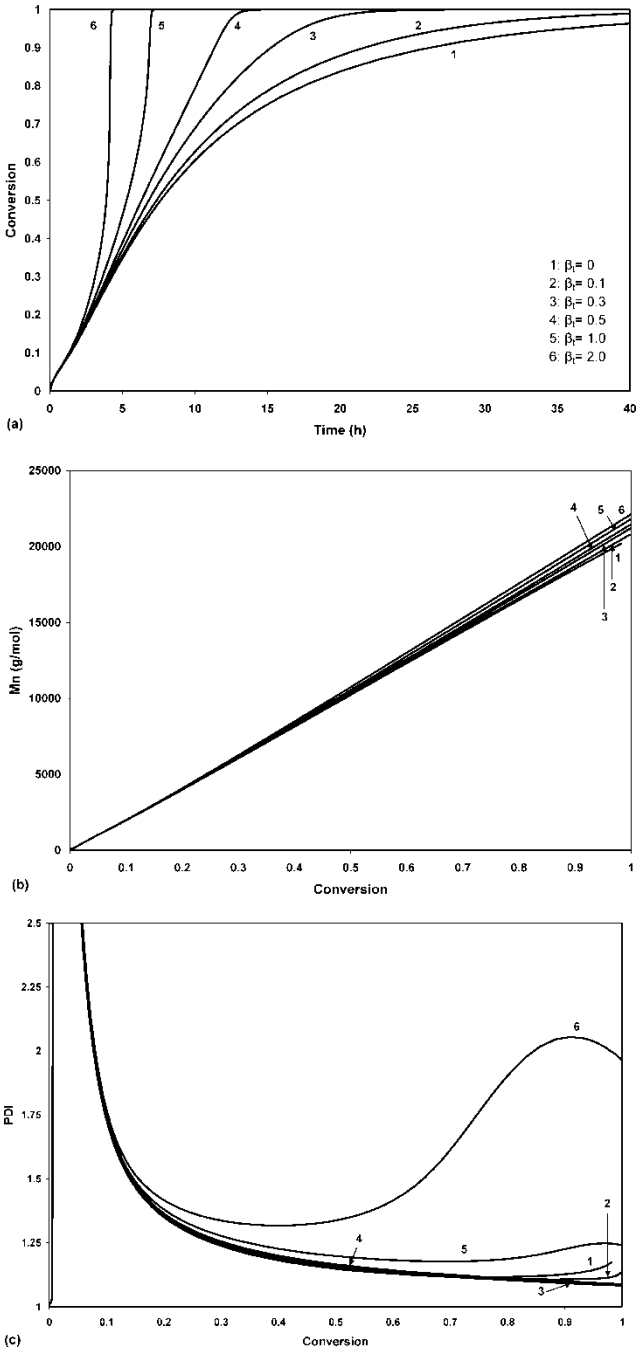

Fig. 1. Effect of diffusion-controlled termination ("gel effect") on (a) monomer conversion vs. time (polymerization rate), (b) number average molecular weight vs. conversion, and (c) PDI vs. conversion, for the NMRP of styrene at 120°C, using TEMPO and BPO at a molar ratio of TEMPO/BPO = 1.1 ($\beta_p = \beta_a = \beta_d = 0$).

4.1 Batch NMRP of Styrene at 120°C Using TEMPO and BPO

Figure 1 shows the effect of DC-termination ("gel effect") on polymerization rate (Figure 1a), number average molecular weight (Figure 1b) and polydispersity index (PDI) (Figure 1c), considering that all the other reactions involving polymer molecules are not diffusion-controlled, namely, $\beta_p = \beta_a = \beta_d = 0$. The cases of non-existent ($\beta_t = 0$) to very strong gel effect ($\beta_t = 2$) were considered. It is observed that although the polymerization rate is very sensitive to the magnitude of the termination free-volume parameter (β_t), the number average molecular weight, M_n, is virtually unaffected by DC termination (only a slight increase on M_n as β_t increases is observed). In the case of PDI, the expected behavior of DC-termination improving the living behavior of the system (PDI tending to a value of one) (20, 21) is observed when weak or moderate DC-effects are considered (profiles 1 to 4 in Figure 1c), but when strong or very strong "auto-acceleration effect" situations are into place (profiles 5 and 6), then PDI increases significantly. For a conventional free-radical polymerization of styrene, $\beta_t = 0.45$ (moderate gel effect), but in the case of ATRP of styrene a much higher value ($\beta_t = 2.12$) has been reported (21). These values contrast with the value ($\beta_t = 0.15$) reported for INIFERTER polymerization of styrene (20). However, it was acknowledged in references (20) and (21) that the experimental data used to estimate β_t in the cases of INIFERTER and ATRP were scarce and did not include data in the high conversion region, where DC effects are known to be especially important.

The case of isolated "glassy effect" (DC propagation, neglecting DC effects of the other reactions) is shown in Figure 2. As observed for other CLRP processes (20, 21), an increase on β_p produced a marked reduction on polymerization rate (Figure 2a), a noticeable reduction on M_n (Figure 2b), and a tendency towards very high PDI values (Figure 2c). This result is expected since reducing the rate of chain growth without altering the rates of chain termination, activation and deactivation reactions, would promote having polymer molecules with a broad chain length distribution.

Figure 3 shows the case when the deactivation of polymer radicals is considered to be diffusion-controlled, assuming that the other reactions are not diffusion-controlled (i.e., $\beta_t = \beta_p = \beta_a = 0$). It is observed that increasing the value of β_d significantly increases the polymerization rate (Figure 3a), and some increase in M_n (Figure 3b) and PDI (Figure 3c) is observed at monomer conversions higher than 70%.

In the case of diffusion-controlled activation of dormant polymer molecules (neglecting DC effects on the other reactions), increasing β_a causes a slight reduction in both polymerization rate (Figure 4a) and M_n (Figure 4b). PDI increases moderately when β_a is increased from 0 to 0.5, but when $\beta_a = 1$, PDI increases sharply from about 50% monomer conversion, reaching a maximum of PDI approximately equal to 4 at about 95% monomer conversion.

In the previous discussion (Figures 1 to 4), the four reactions that could become diffusion-controlled (bimolecular termination, monomer propagation, living polymer deactivation and dormant polymer activation) were analyzed independently of one another, but the fact is that if DC effects are present, they would affect the four reactions simultaneously. The case where moderate DC effects are assumed on all

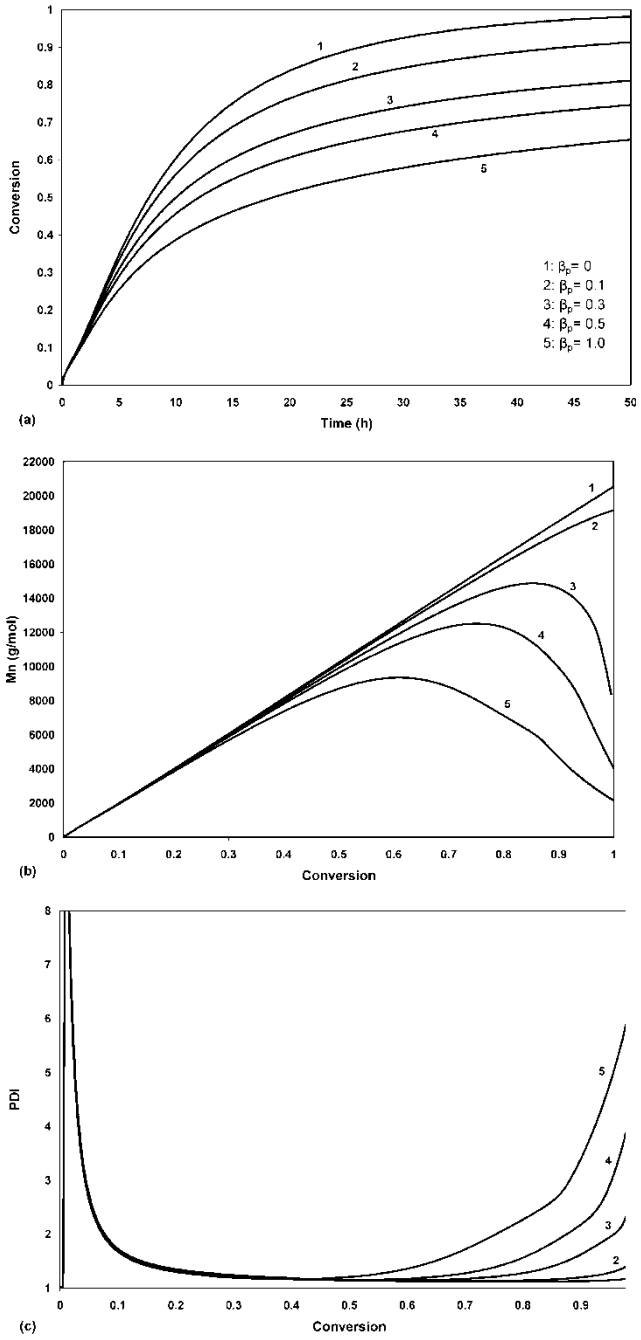

Fig. 2. Effect of diffusion-controlled propagation ("glassy effect") on (a) monomer conversion vs. time (polymerization rate), (b) number average molecular weight vs. conversion, and (c) PDI vs. conversion, for the NMRP of styrene at 120°C, using TEMPO and BPO at a molar ratio of TEMPO/BPO = 1.1 ($\beta_t = \beta_a = \beta_d = 0$).

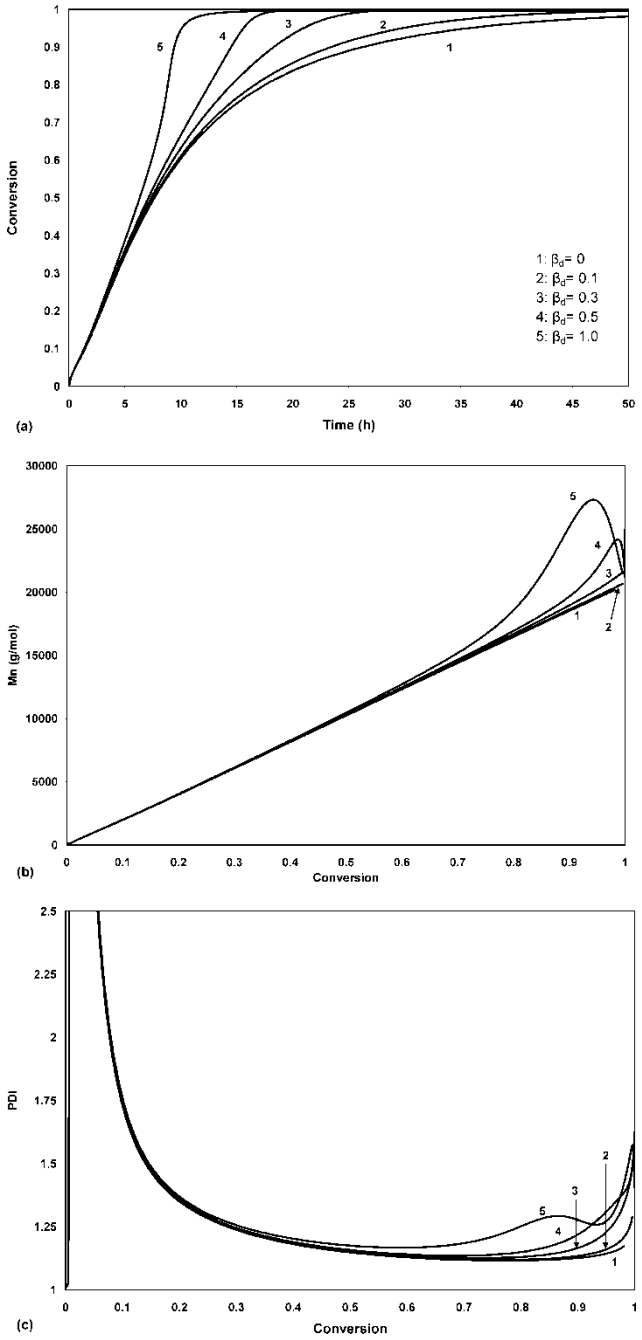

Fig. 3. Effect of diffusion-controlled deactivation on (a) monomer conversion vs. time (polymerization rate), (b) number average molecular weight vs. conversion, and (c) PDI vs. conversion, for the NMRP of styrene at 120°C, using TEMPO and BPO at a molar ratio of TEMPO/BPO = 1.1 ($\beta_t = \beta_p = \beta_a = 0$).

four reactions ($\beta_t = 0.45$, $\beta_p = 0.1$, $\beta_d = 0.1$ and $\beta_a = 0.01$) is shown in Figure 5. The values of β_t and β_p are typical of styrene standard free radical polymerization (32), whereas β_d and β_a were given values based on previous studies on the effects of DC reactions on ATRP (21) and INIFERTER (20) polymerizations of styrene. It is observed in Figure 5a that assuming DC effects on all four reactions causes the polymerization rate to increase significantly, but the profile obtained considering DC-effects deviates from the experimental course (25, 26) even more than the profile obtained without DC effects, which was already slightly above the experimental data at intermediate and high conversions.

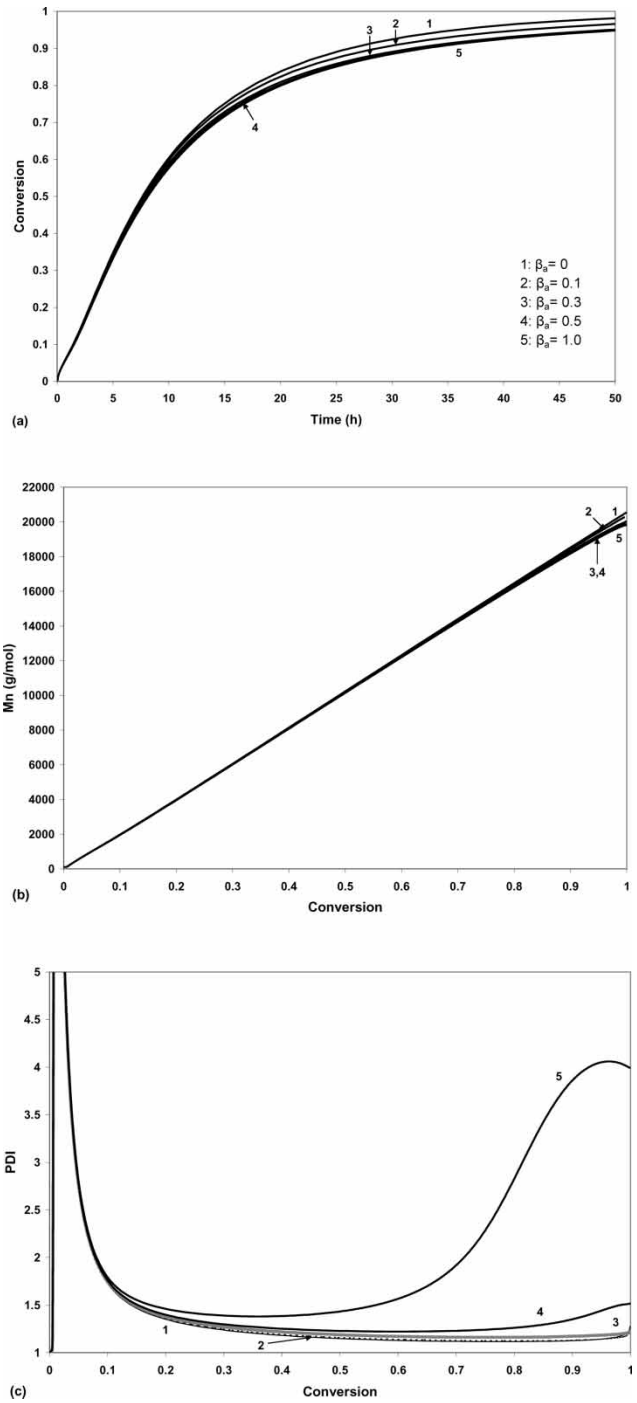

Fig. 4. Effect of diffusion-controlled activation on (a) monomer conversion vs. time (polymerization rate), (b) number average molecular weight vs. conversion, and (c) PDI vs. conversion, for the NMRP of styrene at 120°C, using TEMPO and BPO at a molar ratio of TEMPO/BPO = 1.1 ($\beta_t = \beta_p = \beta_d = 0$).

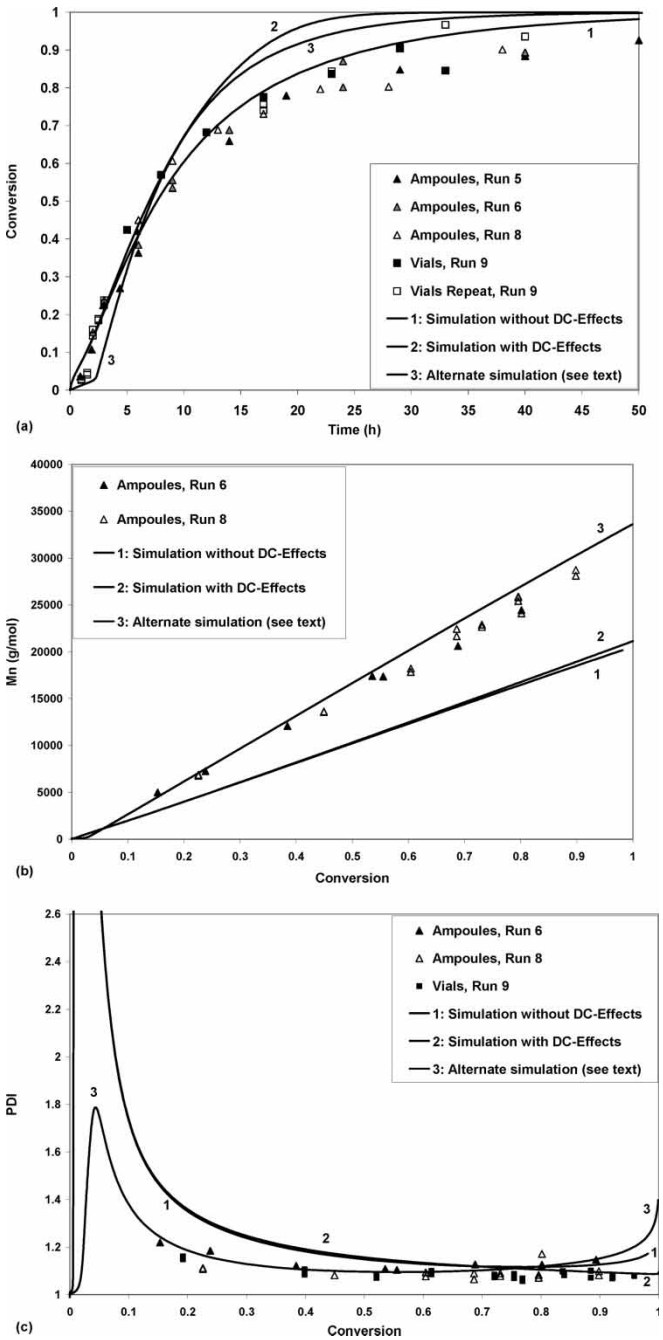

Fig. 5. Effect of combined, moderate, diffusion-controlled effects on (a) monomer conversion vs. time (polymerization rate), (b) number average molecular weight vs. conversion, and (c) PDI vs. conversion, for the NMRP of styrene at 120°C, using TEMPO and BPO at a molar ratio of TEMPO/BPO = 1.1 ($\beta_t = 0.45$, $\beta_p = 0.1$, $\beta_a = 0.01$ and $\beta_d = 0.1$). Experimental data from references (25) and (26), run numbers as in reference (26).

Although the inclusion of DC-effects caused the predicted profile of M_n vs. conversion to increase slightly (Figure 5b), the improvement was almost negligible, and both profiles (with and without DC effects) significantly underestimate the evolution of M_n with monomer conversion. In the case of PDI, the inclusion of DC reactions did not significantly change the predicted profile. A slight reduction in PDI at high conversions was obtained when DC effects were taken into account, but both profiles fit the experimental data equally well, and their difference in performance at

high conversion is well within the experimental error uncertainty, as evident from the repeats (runs 6, 8 and 9 on Figure 5c) carried out in our experimental studies (25, 26).

Discussion about the "alternate" profiles shown in Figure 5(a,b,c) will be provided in subsection 4.3.

Thus far, it seems as if the inclusion of DC effects on the reactions involving polymer molecules in the NMRP of styrene at 120°C, despite corroborating the trends observed in other CLRP polymerizations (20–22) and providing sensible results, was not effective in terms of improving the predictive power of the model developed by Bonilla et al. (17). One possible explanation for that is that our simulations were carried out using the polymerization conditions and kinetic parameters of a styrene polymerization at 120°C. The polymerization temperature is higher than the glass transition temperature (T_g) of polystyrene, and diffusion-controlled effects, particularly the glassy effect, are known to be negligible at those conditions. In the cases of INIFERTER, ATRP and RAFT polymerizations of styrene, DC effects have been found to be more important because those polymerizations are usually carried out at temperatures lower than the T_g of polystyrene.

However, the apparently large effect on polymerization rate during the semi-batch addition of AIBN in the NMRP of styrene at 120°C using TEMPO as controller, also modeled (in a preliminary way) by our group (24), could only be explained in terms of the presence of DC effects on the four reactions considered in this paper. The need to understand why DC effects can be important when a different initiator is added in a semi-batch fashion, even though the monomer, controller and polymerization temperature are the same as in this subsection, motivated the second part of our study.

4.2 Semi-batch NMRP of Styrene at 120°C Using TEMPO and AIBN

The semi-batch addition of AIBN in the NMRP of styrene studied by Díaz-Camacho et al. (24) was modeled using the "Reactors" option of the Predici® "Workshop", which implied creating a user defined file with the times and volumetric amounts of the feed stream, and providing the corresponding concentration of AIBN in the feed (it was assumed that only AIBN was present in the feed shots, namely, the presence of toluene was neglected).

Figure 6 shows the simulated profiles of $\ln([M]_0/[M])$ vs. time. The case where diffusion controlled effects are neglected is shown in Figure 6a. It can be observed that increasing the time between additions (τ), causes a small increase on polymerization rate, much smaller than the one observed experimentally, and certainly no maximum on polymerization rate at $\tau = 60$ min was predicted, as the experimental data shown in Figure 1 of Díaz-Camacho et al. (24) suggest. Contrary to what had been reported in a preliminary simulation study (24), we did not obtain the maximum on polymerization rate at $\tau = 60$ minutes even when DC

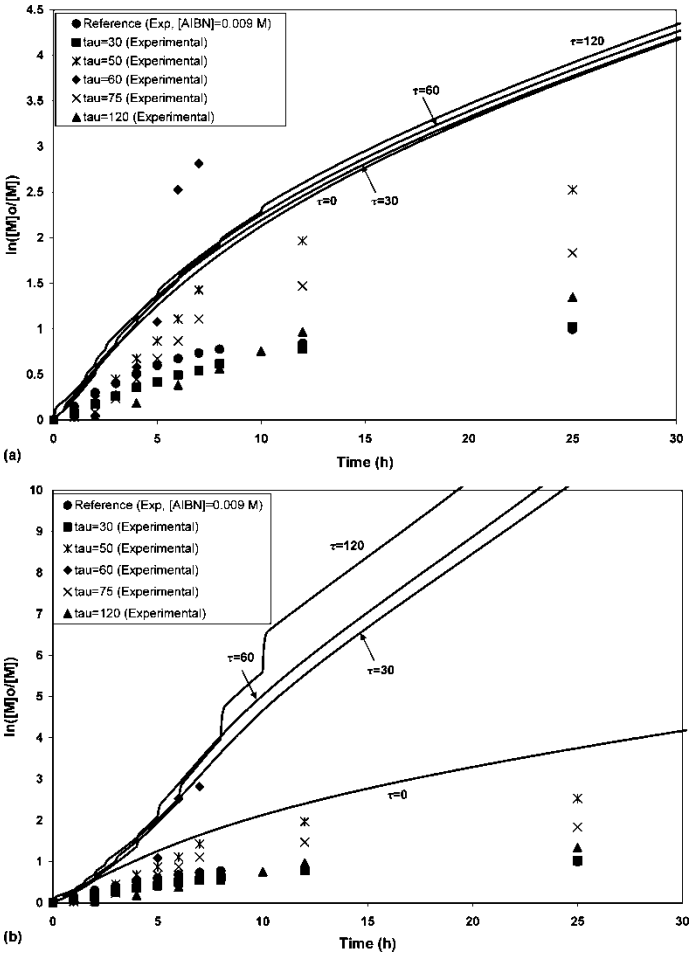

Fig. 6. Comparison of simulated and experimental data of logarithmic conversion vs. time for the NMRP of styrene at 120°C using TEMPO and AIBN, with semi-batch addition of AIBN: (a) simulations without considering DC-effects, and (b) simulations considering DC-effects (the case with $\tau = 0$, without DC-effects, is shown as reference). Free-volume parameters: $\beta_t = 0.45$, $\beta_p = 0.1$, $\beta_a = 0.01$, and $\beta_d = 0.1$.

effects were included in the calculations (Figure 6b), although the differences in polymerization rate are certainly much more pronounced when DC effects are included than when not. As observed in Figure 6a, the polymerization rate when $\tau = 60$ minutes is the fastest from about 6 to 8 h of polymerization time, but when the fourth shot of initiator is added at precisely 8 h, the case with $\tau = 120$ min becomes the fastest one from there on.

Upon careful inspection of the results reported by Díaz-Camacho et al. (24), we found that the profile corresponding to $\tau = 120$ min of Figure 3 of reference (24) (the simulated profiles of Figure 6b in the present study) was mistakenly plotted directly as conversion vs. time, without transforming the data to logarithmic conversion, a situation which coincidentally showed the observed experimental trend. The correct profile is shown in Figure 6b of this study. It is not clear if there was a systematic error in the measurement of

conversion vs. time in the study carried out by Díaz-Camacho et al. (24), which might have caused most of the data to lie below the predicted profiles, or if another phenomenon not captured by the model is occurring when the initiator is added in a semi-batch fashion. Regardless of that, the fact that a much higher polymerization rate than that obtained when BPO is used was observed experimentally in at least one case ($\tau = 60$ min), which agreed with our model predictions, is an indication that high polymerization rates are possible when BPO is replaced by AIBN, an observation which deserved further study.

Figure 7 shows a comparison of model predictions (considering DC effects) and experimental data of M_n vs. conversion (Figure 7a) and PDI vs. conversion (Figure 7b) for the cases with $\tau = 30$ and 60 min. Although the times (conversions) of addition of AIBN are clearly visible in all the profiles, of both M_n and PDI vs. conversion, it is observed that there is an almost negligible effect of the value of τ on the mean value (M_n) and spread (PDI) of the molecular weight distribution. The profiles without DC effects practically overlapped with the ones presented in Figure 7. What seems remarkable about these simulations is that the agreement with the experimental data is good (except for one value of M_n for $\tau = 30$ min at approximately 64% of monomer conversion, which seems to be an outlier). This seemed strange at first, considering that in our previous simulations for the polymerization of styrene with TEMPO and BPO, we could not get good predictions of M_n vs. conversion (our simulated profiles always lie below the experimental data in that polymerization system). It may be possible that our values of k_d or f for BPO could be slightly high, although they were taken from the literature. This issue will be analyzed in more detail in the next subsection.

Figure 8a (left axis) shows the AIBN concentration profiles for the cases $\tau = 0$, 30, 60 and 120 min. It is clearly observed that the initial AIBN (initial concentration of 0.009 M when $\tau = 0$ min and 0.006 M for the other cases) is completely consumed in less than 15 min and the

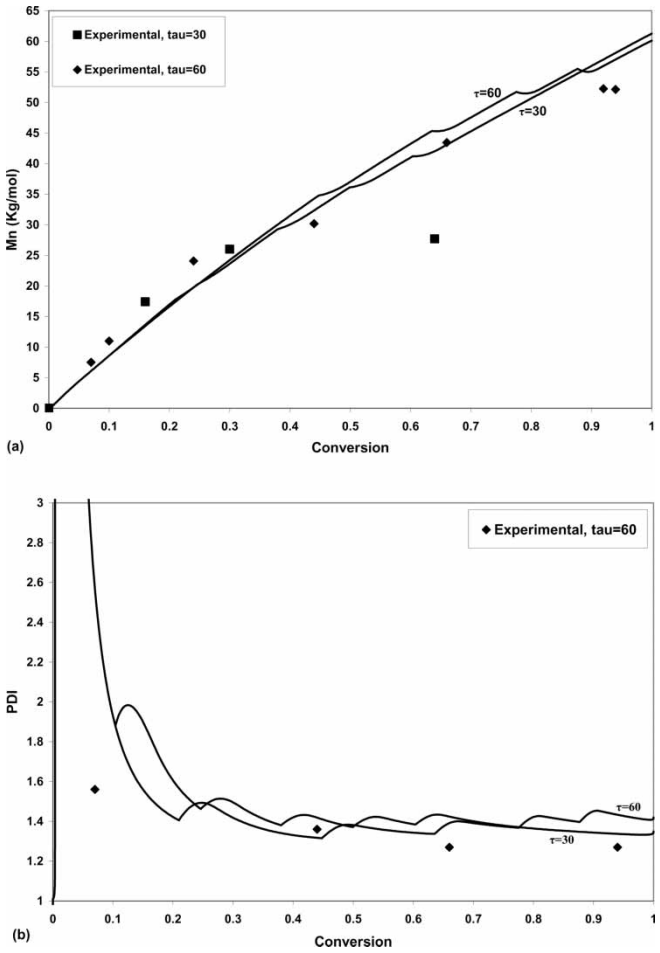

Fig. 7. Effect of time interval of addition (τ) of AIBN and comparison against experimental data (24) in the NMRP of styrene at 120°C: (a) M_n vs. conversion, and (b) PDI vs. conversion. $[AIBN]_0 = 0.006$ mol L^{-1}.

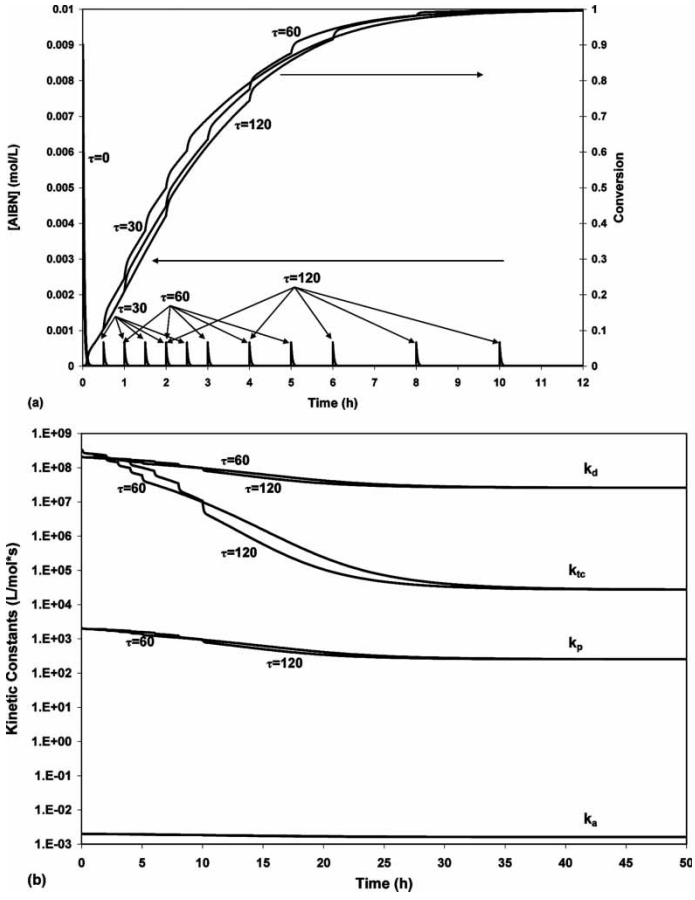

Fig. 8. Semi-batch addition of AIBN in NMRP of styrene at 120°C: (a) initiator concentration and monomer conversion profiles for the reference case ($\tau = 0$), and three addition regimes ($\tau = 30$, 60, and 120 min), and (b) evolution in time of the DC kinetic rate constants (k_{tc}, k_p, k_d and k_a) for $\tau = 60$ and 120 min.

concentration is increased abruptly every τ minutes by the shots of AIBN added. In the same plot, (Figure 8a), the corresponding profiles of conversion vs. time are shown (right axis). It is observed that although the polymerization rate is increased with every addition of AIBN, the overall profiles look very much alike, since the overall amount of AIBN used in all the cases analyzed is the same (the overall concentration of AIBN being 0.009 M once all the shots have been added). Figure 8b shows the evolution with time of the kinetic rate constants that were modeled as diffusion controlled. The decrease of the kinetic rate constants is of course proportional to the free-volume parameters used to model the DC effects. Once again, it is observed that although the shots of AIBN have some effect on the profiles, the overall shape of the profiles does not change significantly.

4.3 A Note on the Importance of Parameter Estimation in Multi-Parameter Nonlinear Models

In our previous analysis of Figure 5 (NMRP of styrene at 120°C using TEMPO and BPO), it was found that the predictions of conversion vs. time (Figure 5a) and PDI vs. conversion (Figure 5c) agreed satisfactorily with our experimental data (25, 26). However, M_n was significantly underestimated, an aspect that was initially thought to be caused by not considering diffusion-controlled effects (which we proved earlier in this paper not to be the case), or to possible side reactions not considered in the model which could deactivate the polymer radicals. However, the facts that the predictions of M_n vs. conversion for the system using AIBN (Figure 7a) were very good, and that the only difference between the two systems was the initiator being used, led us to believe that our estimates of k_d and f, both taken from reference (16), could be inaccurate.

Since the value for k_d reported in Zhang and Ray (16) was not referred to any specific source, and considering that differences of up to two orders of magnitude have been reported in the literature, we decided to use an Arrhenius expression for the "alternate" profile shown in Figure 5, reported by a supplier of chemical initiators (28). There is an order of magnitude difference at 120°C between the values estimated with the two correlations (both of them reported in Table 2). Once k_d had been assigned a new value, it was then decided to try to fit the predicted M_n vs. conversion profile to the experimental data by changing the value of f. It should be emphasized that it has been proposed in the literature that f in NMRP is lower than in conventional free radical polymerization (16), due to the presence of the stable free radicals. An excellent fit was obtained with a value of $f = 0.1$, but the calculated profile of conversion vs. time (not shown in Figure 5) would significantly deviate from the experimental data due to a very large induction time predicted with the model. That effect was compensated by increasing by one order of magnitude (from 0.001 to 0.01 L mol^{-1} s^{-1}), the value of the kinetic rate constant of the "rate enhancement" reaction, k_{h3}. As a matter of fact, a value of $k_{h3} = 0.001$ L mol^{-1} s^{-1} was used by Bonilla et al. (17) and a value of $k_{h3} = 0.01$ L mol^{-1} s^{-1} was used by Belicanta-Ximenes et al. (27), but that difference did not significantly change the original profiles reported in this paper (Figures 1 to 4) with the parameters for BPO from Zhang and Ray (16).

However, since the new calculations (not shown) showed a significant induction period, an increase of one order of magnitude in the value of k_{h3} would significantly reduce that induction period, a behavior also observed by Roa-Luna et al. (26). The new predicted profiles of conversion vs. time (Figure 5a), M_n vs. conversion (Figure 5b) and PDI vs. conversion (Figure 5c) obtained by using $f = 0.1$ and $k_{h3} = 0.01$ are identified in Figure 5 as "alternate" simulations. It is clearly observed that the agreement of molecular weight development with the new values of f and k_{h3} is much better, but the predicted profile of conversion vs. time underestimates the polymerization rate in the low conversion region and overestimates it in the upper conversion region, although the overall agreement in this case is still relatively satisfactory.

This exercise of improving the agreement between simulated profiles and experimental data shows the importance of carrying out adequate parameter estimation procedures, an issue often de-emphasized or even ignored by several research groups. Guidelines about more adequate ways to perform parameter estimation studies have been proposed by Polic et al. (33).

5 Conclusions

The NMRP of styrene with TEMPO and either BPO (batch) or AIBN (added in a semi-batch fashion) at 120°C was modeled considering diffusion-controlled effects on all the reactions with polymer molecules (bimolecular radical termination, monomer propagation, dormant polymer activation or living polymer deactivation), building on a previously developed kinetic model (17). The expected trends observed in previous studies carried out by our group for other CLRP processes (20, 21) were basically the same (DC-termination enhancing the living behavior of the system, while DC-effects on the other reactions worsen it). However, considering that the effects of DC-termination are compensated for by the effects of DC-propagation, DC-activation and DC-deactivation, and that the polymerization temperature used in NMRP polymerizations is relatively high (usually higher that the T_g of the polymer), the overall effect is that DC effects in NMRP are very weak.

Although it was found that considering DC effects in our model for NMRP of styrene using TEMPO and AIBN added intermittently (semi-batch) cannot explain the strong dependence of polymerization rate on the frequency of addition of the shots (τ), as it was believed in a preliminary simulation report (24), the fact that quite high polymerization rates can be obtained when styrene is

polymerized at 120°C using TEMPO and AIBN calls for further scrutiny of the effect of using different initiators in the TEMPO-mediated polymerization of styrene. Some groups have already started the exploration of this issue of studying the effect of the rate of radical generation on polymerization rate and molecular weight development NMRP (34, 35).

6 Nomenclature

[]	Denotes concentration, mol L^{-1}
D	Dimer
$D^{\bullet}$	Dimeric free radical
I	Initiator
f	Initiator efficiency
k_a	Dormant polymer activation kinetic rate constant, s^{-1}
k_d	Kinetic rate constant for initiation decomposition, s^{-1}
k_{da}	Polymer radical deactivation kinetic rate constant, L mol^{-1} s^{-1}
k_{decomp}	Kinetic rate constant for the alcoxyamine decomposition reaction, s^{-1}
k_{dim}	Kinetic rate constant for the dimerization reaction, L mol^{-1} s^{-1}
k_{fD}	Transfer to dimer kinetic rate constant, L mol^{-1} s^{-1}
k_{fm}	Transfer to monomer kinetic rate constant, L mol^{-1} s^{-1}
k_{h3}	Kinetic rate constant for the rate enhancement reaction, L mol^{-1} s^{-1}
k_i	Kinetic rate constant for first propagation reaction, L mol^{-1} s^{-1}
k_p	Propagation kinetic rate constant, L mol^{-1} s^{-1}
k_{tc}	Termination by combination kinetic rate constant, L mol^{-1} s^{-1}
k_{th}	Kinetic rate constant for thermal initiation, L mol^{-1} s^{-1}
HNO_x	Hydroxyl amine
M	Monomer
$M^{\bullet}$	Monomeric free radical
MNO_x	Monomeric alcoxyamine
$NO_x^{\bullet}$	Nitroxyl stable free radical
P_r	Dead polymer molecule of size r
$R_{in}^{\bullet}$	Primary free radical from initiator decomposition
$R_r^{\bullet}$	Polymer free radical of size r
R_rNO_x	Dormant polymer molecule of size r
T	Temperature, K
T_g	Glass transition temperature, K (or °C)
v_f	Fractional free volume
V_i	Volume of species i, L
V_t	System volume, L

6.1 Greek Letters

α_i	Volumetric expansion coefficient, K^{-1}
β_a	Free volume parameter for the activation reaction
β_d	Free volume parameter for the deactivation reaction
β_p	Free volume parameter for the propagation reaction
β_t	Free volume parameter for the termination reaction

7 Acknowledgements

The authors wish to acknowledge financial support from Consejo Nacional de Ciencia y Tecnología (CONACYT) (Project CIAM U40259-Y) (Mexico), Natural Sciences and Engineering Research Council (NSERC) (Canada), and CNPq (Brazil), through a special Inter American Materials Collaboration (IAMC or CIAM) joint project. E. V.-L. gratefully acknowledges DGAPA-UNAM (PASPA Program) and the Department of Chemical Engineering of the University of Waterloo for the financial support received during his research stay at the University of Waterloo. M.R.-L. acknowledges the graduate scholarships for PhD studies from CONACYT and Dirección General de Estudios de Posgrado (DGEP) of UNAM.

8 References

1. Matyjaszewski, K. Controlled/living radical polymerization: state of the art in 2002. In Advances in Controlled/Living Radical Polymerization; Matyjaszewski, K. (ed.), ACS Symposium Series, American Chemical Society: Washington, D.C.; Vol. 854, 2–9, 2003.
2. Pirrung, F.O.H., Quednau, P.H. and Auschra, C. (2002) *Chimia*, **56**, 170.
3. Auschra, C., Eckstein, E., Mühlebach, A., Zink, M.O. and Rime, F. (2002) *Prog. Org. Coat.*, **45**, 83.
4. Pirrung, F.O.H. and Auschra, C. (2005) *ACS Polymer Preprints*, **46(2)**, 316–317.
5. Hawker, C.J. Nitroxide mediated living radical polymerization. In *Handbook of Radical Polymerization*; Matyjaszewski, K. and Davis, T.P. (eds.); John Wiley and Sons, Inc: Hoboken, NJ, 463–522, 2002.
6. Fukuda, T., Goto, A. and Tsujii, Y. Kinetics of living radical polymerization. In *Handbook of Radical Polymerization*; Matyjaszewski, K. and Davis, T.P. (eds.); John Wiley and Sons, Inc: Hoboken, NJ, 407–462, 2002.
7. Goto, A. and Fukuda, T. (2004) *Prog. Polym. Sci.*, **29**, 329–385.
8. Fukuda, T., Terauchi, T., Goto, A., Ohno, K., Tsujii, Y., Miyamoto, T., Kobatake, S. and Yamada, B. (1996) *Macromolecules*, **29**, 6393–6398.
9. Yoshikawa, C., Goto, A. and Fukuda, T. (2002) *Macromolecules*, **35**, 5801–5807.
10. Fischer, H. (2001) *Chem. Rev.*, **101**, 3581–3610.
11. Fischer, H. and Tordo, P. (2002) *Macromol. Symp.*, **182**, 225.
12. Souaille, M. and Fischer, H. (2001) *Macromolecules*, **34**, 2830.
13. Souaille, M. and Fischer, H. (2002) *Macromolecules*, **35**, 248–261.

14. Fischer, H. Chapter 3. In *Advances in Controlled/Living Radical Polymerization*; Matyjaszewski, K. (ed.), ACS Symposium Series 854, American Chemical Society: Washington, D.C., 2003.
15. Saldívar-Guerra, E., Bonilla, J., Becerril, F., Zacahua, G., Albores-Velasco, M., Alexander-Katz, R., Flores-Santos, L. and Alexandrova, L. (2006) *Macromol. Theory Simul.*, **15**, 163–175.
16. Zhang, M. and Ray, W.H. (2002) *J. Appl. Polym. Sci.*, **86**, 1630–1662.
17. Bonilla, J., Saldívar, E., Flores-Tlacuahuac, A., Vivaldo-Lima, E., Pfaendner, R. and Tiscareño-Lechuga, F. (2002) *Polym. React. Eng.*, **10(4)**, 227–263.
18. Butté, A., Storti, G. and Morbidelli, M. (1999) *Chem. Eng. Sci.*, **54**, 3225–3231.
19. Faliks, A., Yetter, R.A., Floudas, C.A., Wei, Y. and Rabitz, H. (2001) *Polymer*, **42**, 2061–2065.
20. Vivaldo-Lima, E. and Mendoza-Fuentes, A.J. (2002) *Polym. React. Eng.*, **10(4)**, 193–226.
21. Delgadillo-Velázquez, O., Vivaldo-Lima, E., Quintero-Ortega, I.A. and Zhu, S. (2002) *AIChE J.*, **48(11)**, 2597–2608.
22. Wang, A.R. and Zhu, S. (2003) *Macromol. Theory Simul.*, **12**, 196–208.
23. Peklak, A.D., Butté, A., Storti, G. and Morbidelli, M. (2006) *J. Polym. Sci., A: Polym. Chem.*, **44**, 1071–1085.
24. Díaz-Camacho, F., López-Morales, S., Vivaldo-Lima, E., Saldívar-Guerra, E., Vera-Graziano, R. and Alexandrova, L. (2004) *Polym. Bull.*, **52**, 339–347.
25. Tuinman, E., McManus, N.T., Roa-Luna, M., Vivaldo-Lima, E., Lona, L.M.F. and Penlidis, A. (2006) *J. Macromol. Sci., A: Pure Appl. Chem.*, **43(7)**, 995–1011.
26. Roa-Luna, M., Nabifar, A., Díaz-Barber, M.P., McManus, N.T., Vivaldo-Lima, E., Lona, L.M.F. and Penlidis, A. (2006) Another Perspective on the Nitroxide Mediated Radical Polymerization (NMRP) of Styrene using 2,2,6,6-Tetramethyl-1-piperidinyloxy (TEMPO) and Dibenzoyl Peroxide BPO submitted to *J. Macromol. Sci., A: Pure Appl. Chem.*, **44**, 2006.
27. Belicanta-Ximenes, J., Mesa, P.V.R., Lona, L.M.F., Vivaldo-Lima, E., McManus, N.T. and Penlidis, A. (2006) Simulation of styrene polymerization by monomolecular and bimolecular nitroxide-mediated radical processes over a range of reaction conditions, submitted to *Macromol Theory Simul*, 2006.
28. Akzo Nobel Chemicals Inc., "Initiators for High Polymers", Chicago, IL, USA, June 2006, pp 16–19 (http://www.akzonobel-polymerchemicals.com/NR/rdonlyres/C2D64A96-B539-4769-A688-2447258D3DCA/0/InitiatorsforHighPolymersAkzoNobel 2006.pdf, last accessed July 30, 2006).
29. Buback, M., Gilbert, R.G., Hutchinson, R.A., Klumperman, B., Kuchta, F.-D., Manders, B.G., O'Driscoll, K.F., Russell, G.T. and Schweer, J. (1995) *Macromol. Chem. Phys.*, **196**, 3267–3280.
30. Buback, M., Kowollik, C., Kurz, C. and Wahl, A. (2000) *Macromol. Chem. Phys.*, **201**, 464–469.
31. Goto, A., Terauchi, T., Fukuda, T. and Miyamoto, T. (1997) *Macromol. Rapid Commun.*, **18**, 673–681.
32. Vivaldo-Lima, E., Hamielec, A.E. and Wood, P.E. (1994) *Polym. React. Eng.*, **2(1&2)**, 17–85.
33. Polic, A.L., Lona, L.M.F., Duever, T.A. and Penlidis, A. (2004) *Macromol. Theory Simul.*, **13**, 115–132.
34. Goto, A. and Fukuda, T. (1997) *Macromolecules*, **30**, 4272.
35. Tobita, H. (2006) *Macromol. Theory Simul.*, **15**, 23–31.